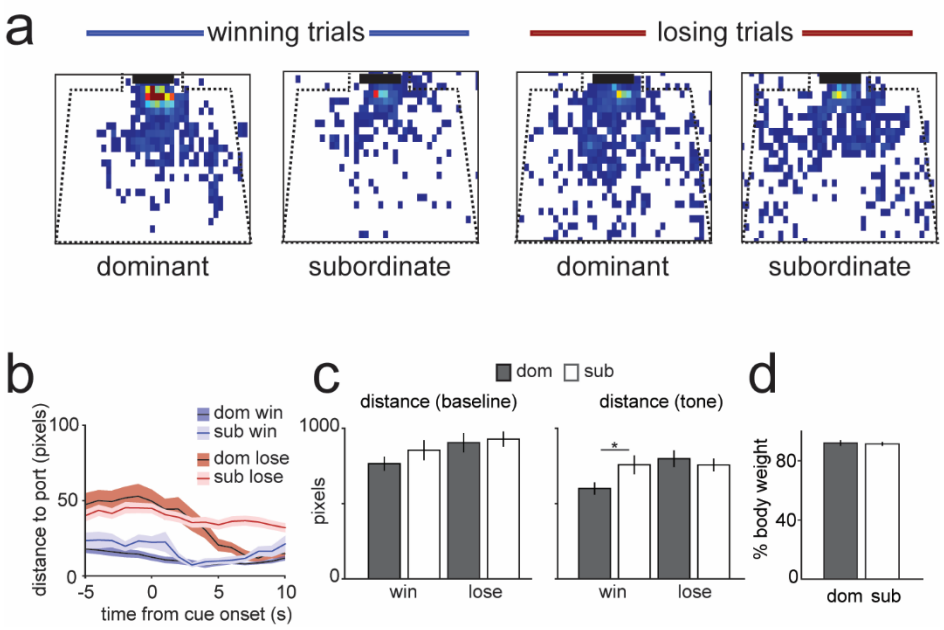

Extended Data 1: Reward location and locomotion by relative rank during the reward competition

a. Area occupied by dominants or subordinates in the 10 seconds prior to the tone onset for *win* vs *lose* trials.

b. Distance to reward port differed by trial type but not by rank (trials n: *dom win*=68, *dom lose*=24, *sub win*=24, *sub lose*=68; 2-way ANOVA rank and trial type; main effect of trial type $F_{(1,180)}=68$, $p=2.5\times10^{-14}$, rank p=0.071, interaction p=0.79).

c. Total distance traveled immediately before the tone and during the tone period (baseline:10 seconds prior to tone; tone: 10 seconds of the tone) across trial types for dominant and subordinate mice (*dom win* n=126, *dom lose* n=71, *sub win* n=71 trials, *sub lose* n=126; Wilcoxon rank-sum, *baseline win* p=0.12, *baseline lose* p=0.31, *tone win* p=0.005, *tone lose* p=0.54).

d. Percent body weight during food restriction did not differ across relative dominant and subordinate mice competing in reward competition (n=12 dyads, paired t-test, p=0.23).

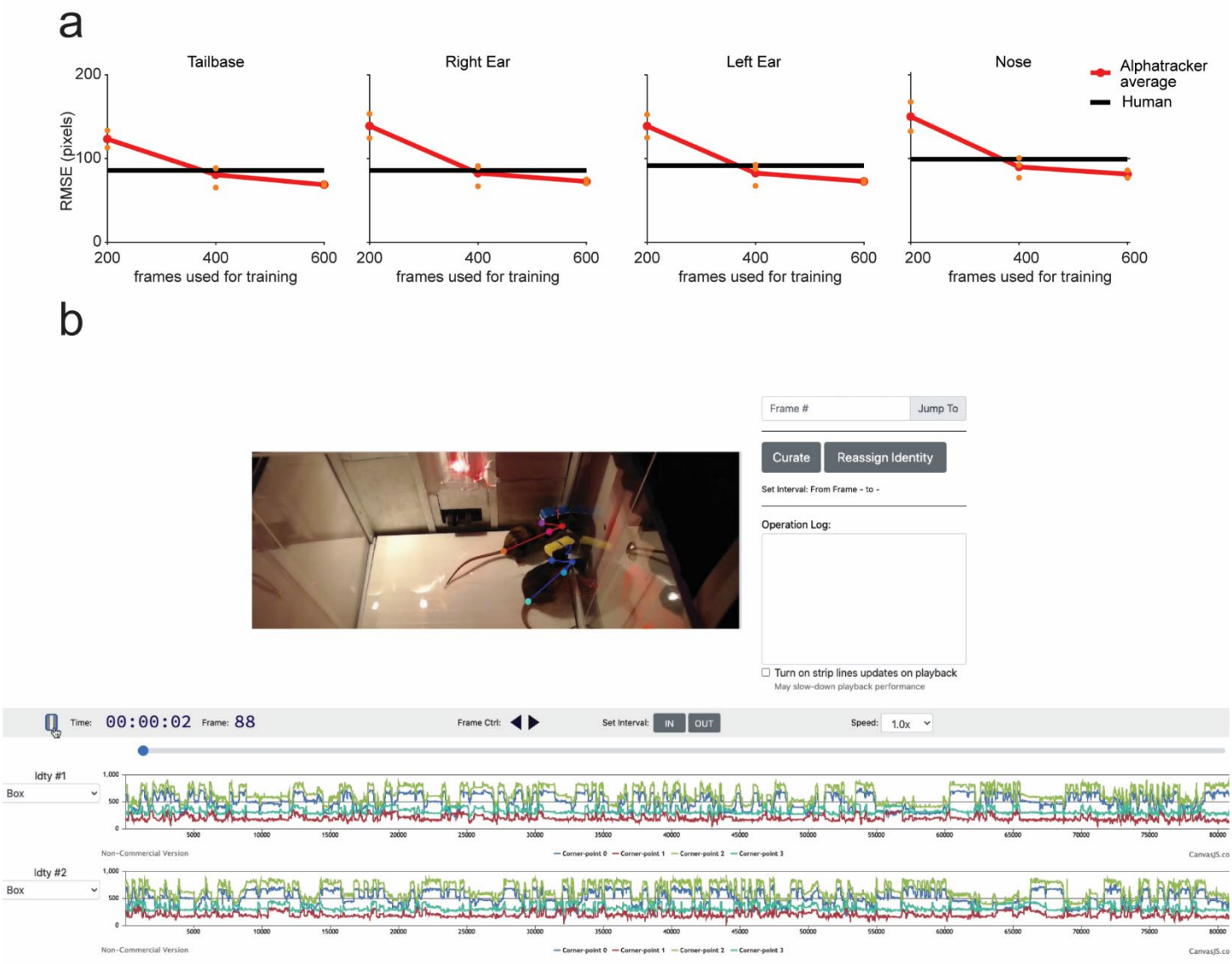

Extended Data 2: AlphaTracker tracking metrics

a. Root mean square error (RMSE) of AlphaTracker when tracking different body parts compared to human level RMSE in videos with high resolution (1920x1080 pixels). Orange dots represent different training/testing iterations with different frames and the red line is the average across iterations.

b. Screenshot of user interface (UI) to fix errors made by AlphaTracker tracking. In addition, this UI can be used for exploring the clustering data.

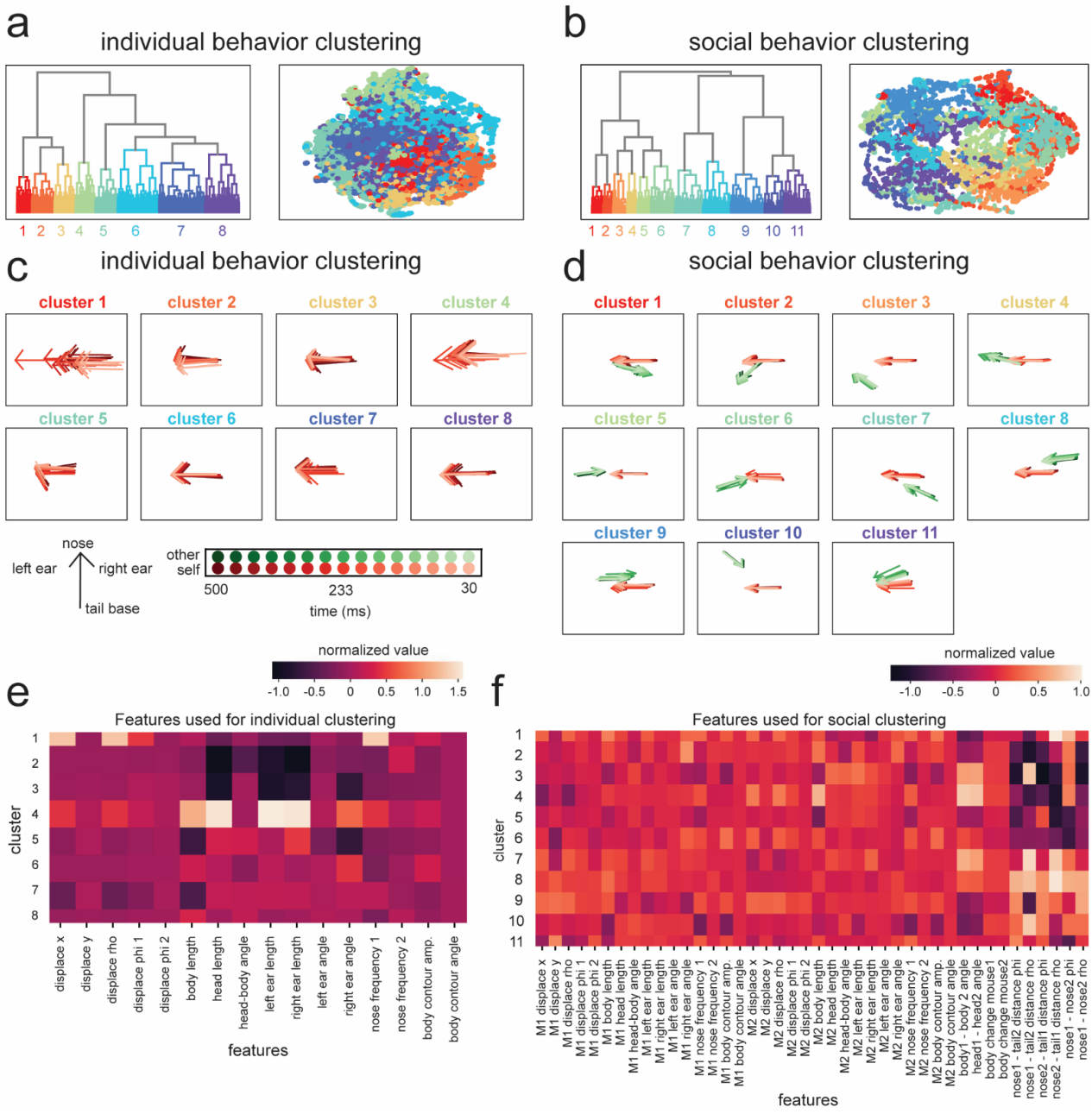

Extended Data 3: AlphaTracker unsupervised clustering results

a. Dendrogram and UMAP plot showing all video clips color coded by cluster ID for individual behavior clustering. Data for this clustering are shown in (c) and features used are shown in (e).
b. Dendrogram and UMAP plot showing all video clips color coded by cluster ID for social behavior clustering. Data for this clustering are shown in (d) and features used are shown in (f).
c. Average normalized skeleton for nose, ears and tail base across clusters for the individual behavior clustering across 500 ms of video clip time.
d. Average normalized skeleton for nose, ears and tail base across clusters for the social behavior clustering across 500 ms of video clip time. Red arrow indicates *self* skeleton and green indicates the *other* skeleton.
e. Heatmap of normalized values for the *self* features used for individual behavior clustering.
f. Heatmap of normalized values for the *self* and *other* features used for social behavior clustering.

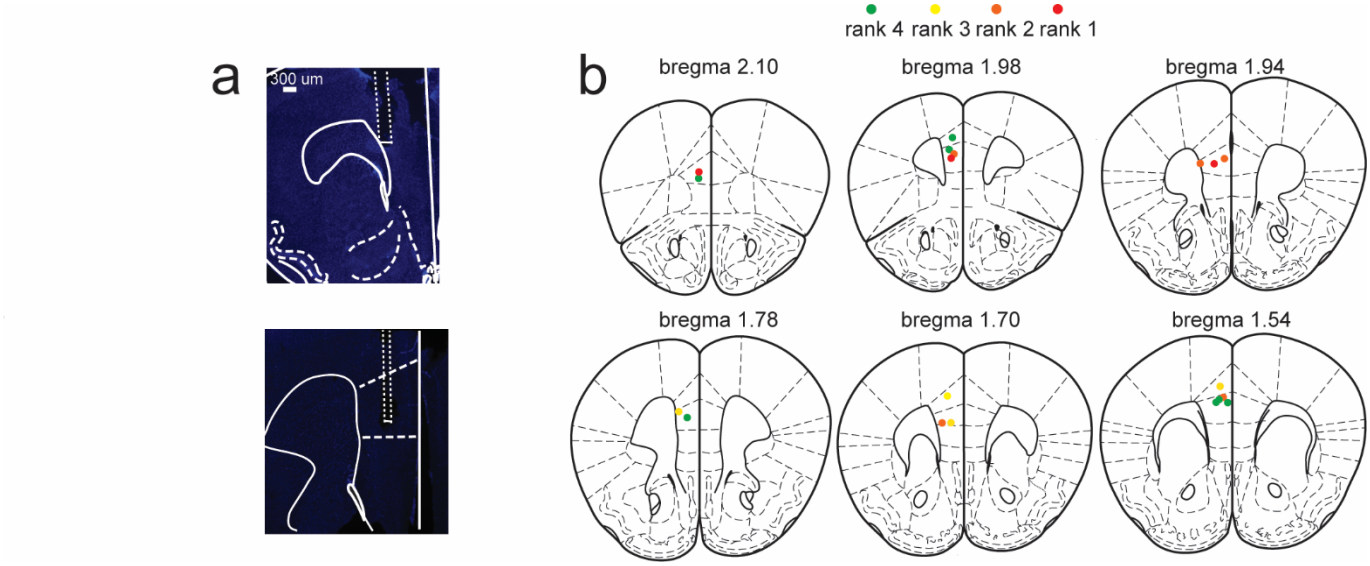

Extended Data 4: mPFC recording sites

a. Representative images showing electrode track and lesions of mPFC electrode wires.
b. Location of center for electrode lesions for all mice color coded by absolute rank across animals.

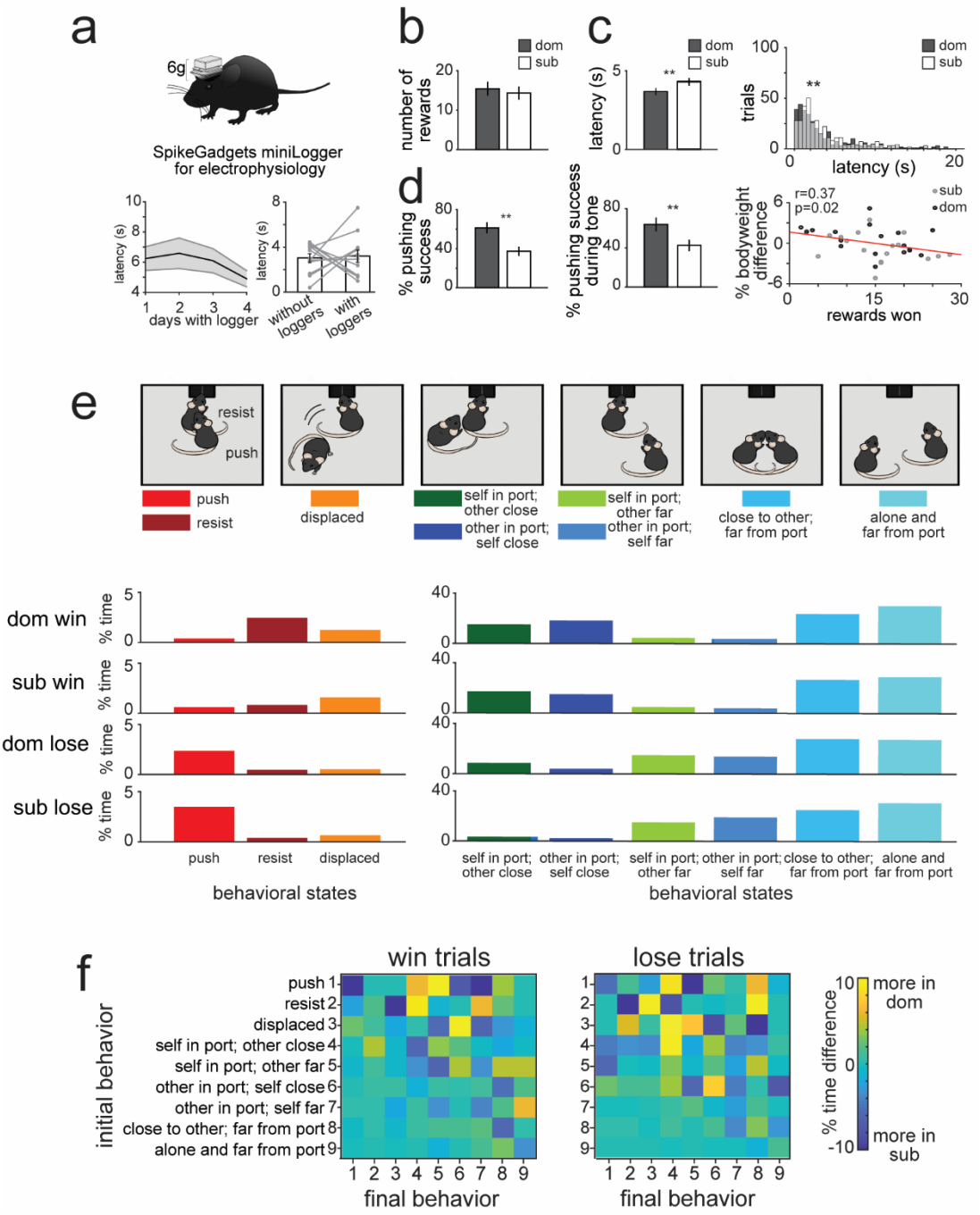

Extended Data 5: Reward competition during wireless recording

a. Left, diagram of wireless electrophysiology recording device (logger) used for mPFC recordings. Right, latency to collect reward while performing reward task alone was not affected by wearing the logger (n=12 mice; paired t-test, p=0.83).

b. Number of rewards obtained by relative dominants (dom) and subordinates (sub) during the reward competitions between animals wearing loggers (n=18 competition sessions; paired t-test, p=0.71).

c. Subordinates had slower latencies to pick up the reward during *win* trials. Left, latency per group. Right, histogram of the distribution of latencies across all trials (*dom trials* n=326, *sub trials* n=358, Wilcoxon rank-sum, p=0.012; Two-sample Kolmogorov-Smirnov test, *dom* vs sub *trials* p=0.015).

d. Left, dominants were more successful displacing subordinates from the reward port throughout the competition (left; n=32 sessions, paired t-test, p=0.002) and during the tone time (middle; n=32 sessions, paired t-test, p=0.005). Right, body weight difference between competitors

significantly correlates with rewards won independent of rank (n=18 sessions, Pearson's correlation, *p=0.02).

e. Distribution of time (normalized by total time) in each of the 9 behaviors analyzed for *win* and *lose* trials separated by relative social rank.
f. Time difference between dominant and subordinates for behavioral transitions during *win* trials (left) vs *lose* trials (right).

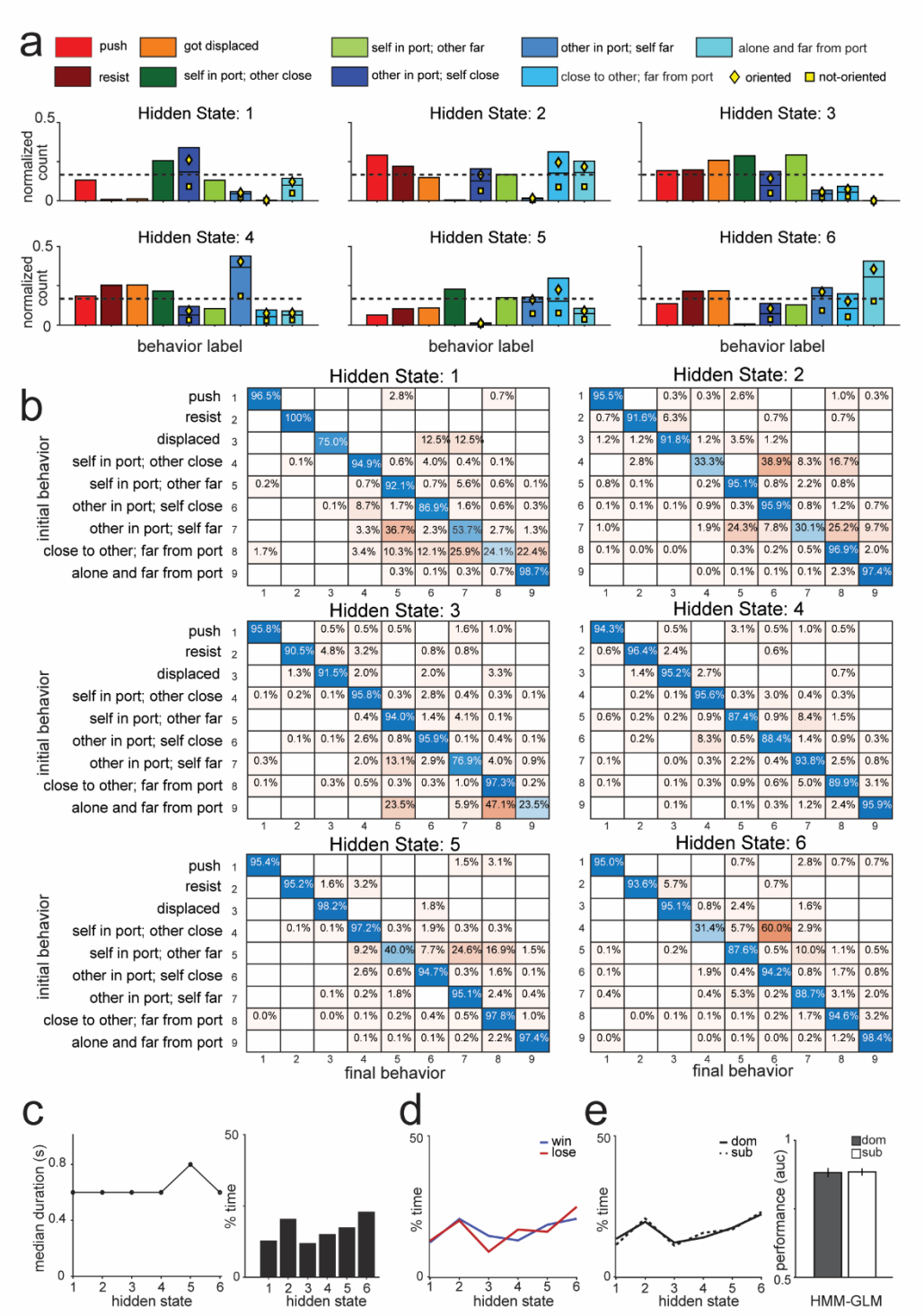

Extended Data 6: Description of social behaviors across HMM-GLM hidden states

a. Distribution of time in each behavioral state across the six hidden states. Each behavior is normalized across clusters by total time for the behavior. Dashed line indicates chance distribution across the six hidden states. Oriented vs not oriented refers to times when mouse is looking towards or away from the port.
b. Transitions between behaviors in each of the six hidden states. Percent time in each transition for each initial behavior is indicated in each plot.
c. Left, mean duration and right, percent time spent in each hidden state.
d. Percent time in each hidden state separated by competitive success.

e. Left, percent time in each hidden state separated by rank. Right, performance of six state HMM-GLM decoding behavioral states does not differ across social rank (n=9 behavioral states; Wilcoxon rank-sum, p=0.86).

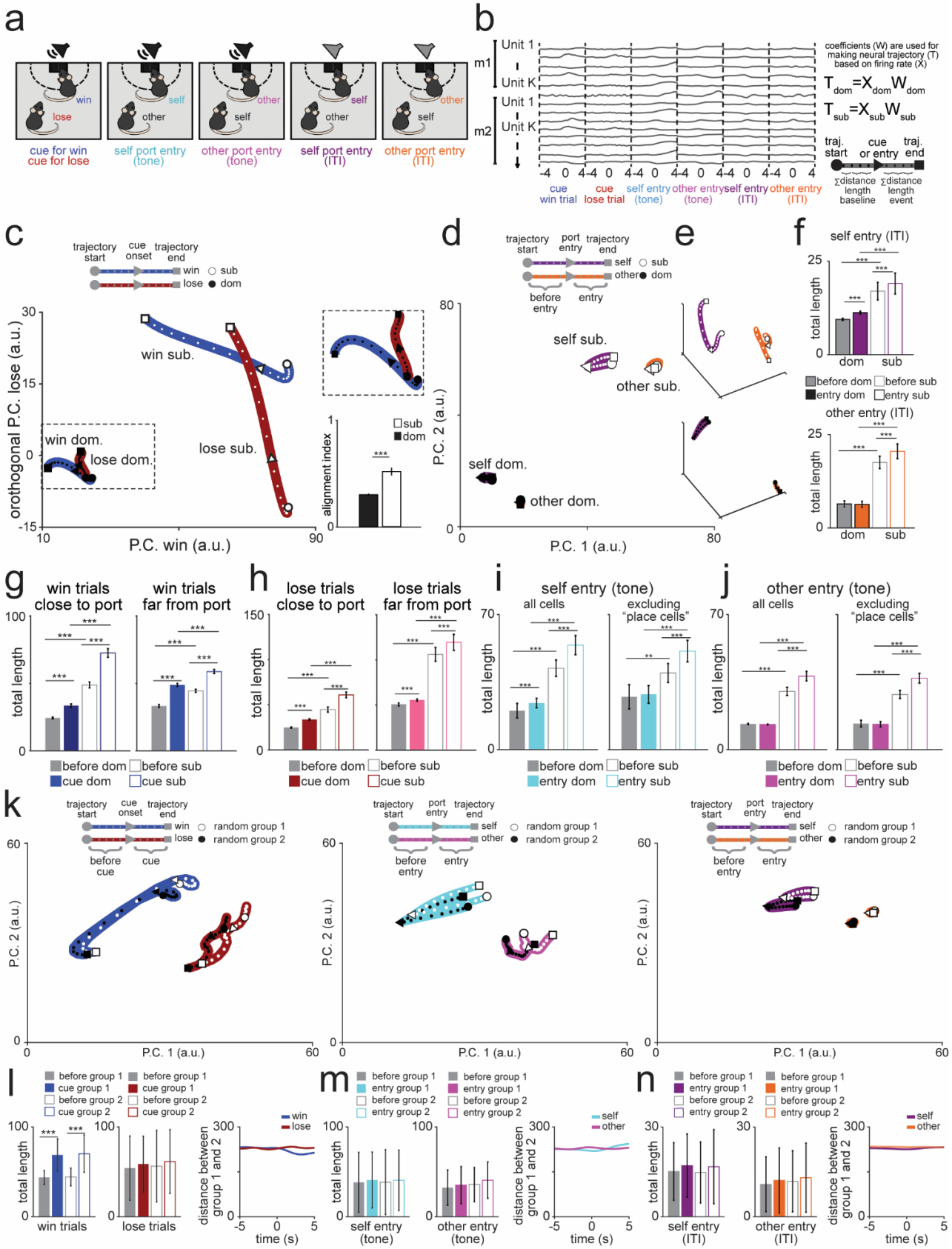

Extended Data 7: Additional data for mPFC population dynamics during social competition

a. Depictions of task-relevant events: *win* and *lose* trials and all types of port entries used for analyses.

b. Data arrangement across all animals (m1=mouse 1, m2=mouse 2) for the dimensionality reduction to a common subspace for the six task-relevant events. Neural trajectories were

created for dominant and subordinate data using mean firing rate per event and the principal component analysis coefficients. Right, diagram explaining distance and length metrics for neural trajectory analysis.

c. Left, neural trajectories for *win* and *lose* trials plotted in the first Principal Component (PC) for *win* and the orthogonal *lose* subspace show little overlap. Top right, inset of dominant neural trajectories. Bottom right, alignment of *win* and *lose* trajectories was significantly lower for dominant mice (Wilcoxon rank-sum, $p=1.5x10^{-5}$).

d. Neural trajectories of mPFC population firing rate during inter-trial interval (ITI) *port entries* projected into the first two principle components of the common behavioral subspace.

e. Neural trajectories from in (d) plotted in 3D to facilitate visualization.

f. Neural trajectory lengths for *self entry* (top) and *other entry* (bottom) during the ITI (*self entry*: 2-way ANOVA main effect of rank $F_{(1,50)}=72.3$, $p=2x10^{-11}$, event $F_{(1,50)}=4.4$, $p=0.03$; *other entry*: 2-way ANOVA main effect of rank $F_{(1,50)}=325$, $p=1x10^{-23}$, event $F_{(1,50)}=4.1$, $p=0.04$ and interaction $F_{(1,50)}=31$, $p=0.03$).

g. To determine if distance to reward port affected the population dynamics during *win* and *lose* trials a subset of data with matched video settings was split by distance to reward port. Neural trajectory lengths were higher for dominants during *win* trials in which mice were close and far to the reward port at tone onset (*win close to port*: 2-way ANOVA main effect of rank $F_{(1,70)}=985$, $p=5x10^{-43}$, event $F_{(1,70)}=263$, $p=1x10^{-25}$ and interaction $F_{(1,70)}=52$, $p=4x10^{-10}$; *win far from port*: 2-way ANOVA main effect of rank $F_{(1,70)}=296$, $p=7x10^{-27}$, event $F_{(1,70)}=596$, $p=5x10^{-36}$).

h. Neural trajectory lengths were higher for dominants during *lose* trials in which mice were c*lose* and far from reward port at the onset of the tone (*lose close to port*: 2-way ANOVA main effect of rank $F_{(1,70)}=484$, $p=3x10^{-33}$, event $F_{(1,70)}=136$, $p=4x10^{-18}$ and interaction $F_{(1,70)}=11$, $p=9x10^{-4}$; *lose far from port*: 2-way ANOVA main effect of rank $F_{(1,70)}=409$, $p=5x10^{-31}$, event $F_{(1,70)}=9.5$, $p=0.002$).

i. To determine if reward "place cells" contributed to neural trajectory differences we calculated the neural trajectory lengths with and without cells that were correlated to distance to port in a subset of data with equivalent video settings (see methods). Left, neural trajectories for *self entry* during the tone are highest for subordinate mice with all cells included and without the distance correlated cells (all cells: 2-way ANOVA main effect of rank $F_{(1,70)}=169$, $p=2x10^{-20}$, event $F_{(1,70)}=15$, $p=0.00001$ and interaction $F_{(1,70)}=4.02$, $p=0.048$; excluding correlated cells: 2-way ANOVA main effect of rank $F_{(1,68)}=40$, $p=2x10^{-8}$, event $F_{(1,68)}=5.2$, $p=0.02$).

j. Same procedure as in (g) for neural trajectories for *other entry* during the tone. Left, neural trajectories are highest for subordinate mice with all cells included and without the distance correlated cells (all cells: 2-way ANOVA main effect of rank $F_{(1,70)}=662$, $p=2x10^{-37}$, event $F_{(1,70)}=21$, $p=1x10^{-5}$ and interaction $F_{(1,70)}=25$, $p=3x10^{-6}$; excluding correlated cells: 2-way ANOVA main effect of rank $F_{(1,68)}=388$, $p=7x10^{-30}$, event $F_{(1,68)}=16$, $p=0.00004$ and interaction $F_{(1,68)}=19$, $p=3x10^{-5}$).

k. Neural trajectories of mPFC population activity for two randomly selected halves of the data for (left) *win* and *lose* trials, (middle) port entries during the tone and (right) ITI port entries. All trajectories reflect the mean trajectories across 50 bootstrapping iterations.

l. Left, trajectory lengths for *win* and *lose* trials when data is divided randomly show only an effect of cue, but not of group (*win*: 2-way ANOVA, event $F_{(1,196)}=154$, $p=1x10^{-26}$, group $F_{(1,196)}=2.46$, $p=0.11$, interaction $F_{(1,196)}=0.38$, $p=0.53$; *lose*: event $F_{(1,196)}=129$, $p=1x10^{-23}$, group $F_{(1,196)}=1.86$, $p=0.17$, interaction $F_{(1,196)}=0.09$, $p=0.75$). Right, mean trajectory distances between groups for *win* and *lose* trials.

m. Left, trajectory lengths for port entries during the tone when data is divided randomly show no difference of group or entry (*self entry*: 2-way ANOVA, event $F_{(1,196)}=0.34$, $p=0.55$, group $F_{(1,196)}=1.86$, $p=0.17$, interaction $F_{(1,196)}=0.004$, $p=0.94$; *other entry*: event $F_{(1,196)}=0.43$, $p=0.51$, group $F_{(1,196)}=1.16$, $p=0.28$, interaction $F_{(1,196)}=0.005$, $p=0.94$). Right, mean trajectory distances between groups for *self entry* and *other entry* during the tone.

n. Left, trajectory lengths for ITI port entries when data is divided randomly show only an effect of entry, but not of group (*self entry*: 2-way ANOVA, event $F_{(1,196)}=18.2$, $p=2x10^{-5}$, group $F_{(1,196)}=0.37$, $p=0.54$, interaction $F_{(1,196)}=0.00002$ $p=0.99$; *other entry*: event $F_{(1,196)}=21.1$, $p=7x10^{-6}$, group $F_{(1,196)}=2.0$, $p=0.15$, interaction $F_{(1,196)}=0.18$, $p=0.66$). Right, mean trajectory distances between groups for *self entry* and *other entry* during the ITI.

Error bars for (c-f) indicate the 95% confidence intervals calculated with the leave-one-out method leaving out one animal at a time. Error bars for (g-j) for indicate 95% confidence intervals obtained with the leave-one-out method leaving out one session at a time. Error bars in (l-n) indicate 95% confidence intervals obtained from 50 bootstrapping iterations with two randomly-assigned groups. All post hoc tests consistent on Bonferroni corrected paired or unpaired t-test **p<.01, ***p<.001.

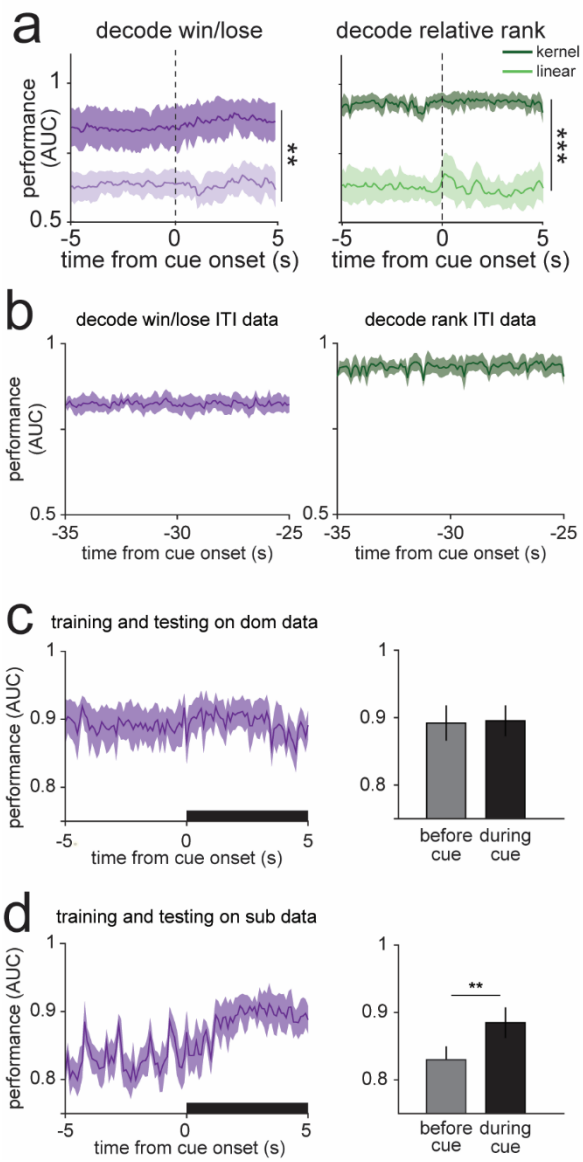

Extended Data 8: Decoding social rank from ITI data and decoding competitive success within a rank.

- **a.** Decoding performance (area under the receiving operating curve; AUC) was higher for SVM with kernel vs linear SVM. A kernel SVM performed better than a linear SVM for decoding competitive success and rank (n=10 fold validation using 1,410 trials; Wilcoxon sign-rank, *win/lose* p=0.001, rank p=0.0002).
- **b.** Decoder performance for classifying competition outcome or rank from data during the intertrial intervals.
- **c.** Decoder performance for classifying competition outcome using training and testing data from dominant mice single units only. Right, the decoder has the same performance during baseline and tone period (n=10 fold validation from 697 trials; Wilcoxon sign-rank, p=0.92).
- **d.** Decoder performance for classifying competition outcome using training and testing data from subordinate mice single units only. Right, decoder performance increased during the tone period (n=10 fold validation from 713 trials; Wilcoxon sign-rank, p=0.002).
  All error bars indicate 95% confidence intervals from 10-fold cross-validation.

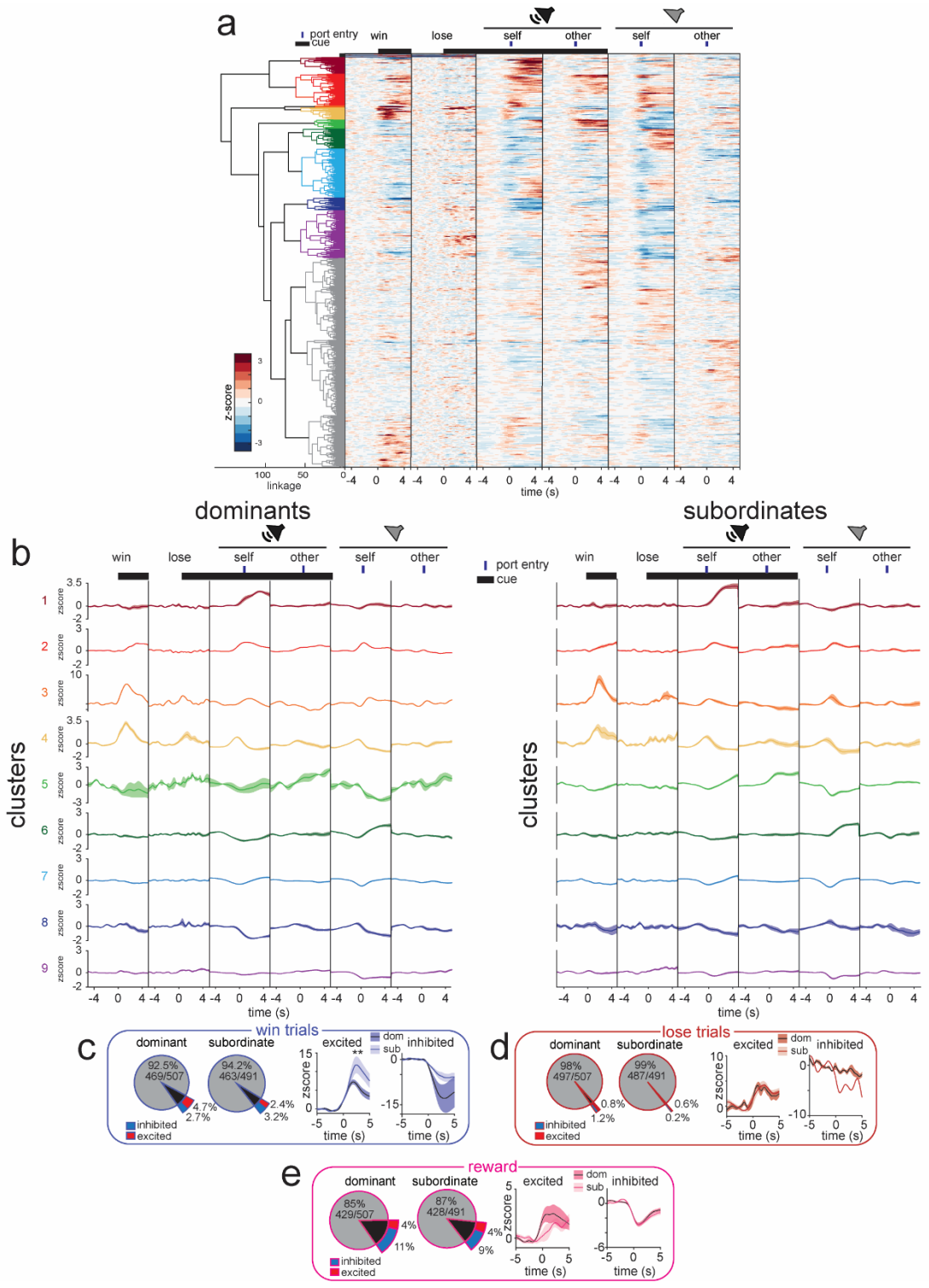

Extended Data 9: Additional data for mPFC single unit responses to task-relevant events during social competition

a. Dendrogram for functional clusters and heatmap of mean firing rate for all the neurons included in the hierarchical clustering (n=998). Gray cells in the dendrogram indicate cells in functional clusters that did not meet criteria of mean z-score being higher than 2 or lower than -1 for at least one event.

b. Mean firing rate for all functional clusters separated by relative rank (left dominant; right subordinate).

c. Left, percent of responsive cells to *win* trials did not differ by relative rank (*dom* n=38/507, *sub* n=28/491; Fisher's exact test, total responsive p=0.30). Right, response magnitude to the cue

for significantly excited cells during *win* trials was higher for subordinates (Wilcoxon rank-sum: excited p=0.01; inhibited p=0.06).

d. Left, percent of responsive cells to *lose* trials did not differ by relative rank (*dom* n=10/507, *sub* n=4/491; Fisher's exact test, total responsive p=0.17). Right, response magnitude to the cue for losing trials did not differ by rank (Wilcoxon rank-sum: excited p=0.62; inhibited p=0.28).
e. Left, percent of responsive cells to the reward consumption did not differ by relative rank (*dom* n=78/507, *sub* n=63/491; Fisher's exact test, total responsive p=0.27). Right, response magnitude to reward consumption did not differ by rank (Wilcoxon rank-sum: excited p=0.72; inhibited p=0.15).

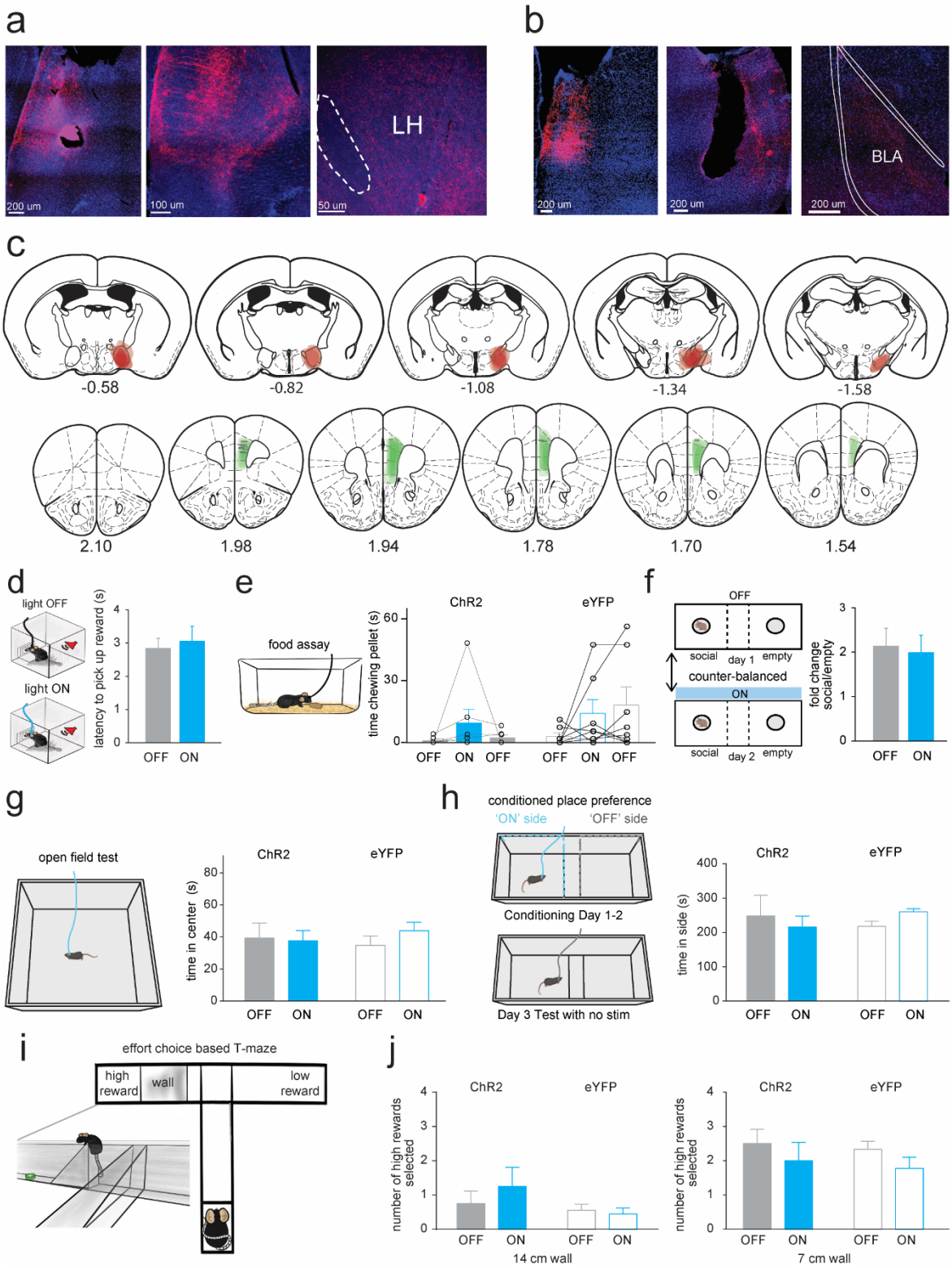

Extended Data 10: mPFC-LH photostimulation does not affect other motivated behaviors

a. Representative images showing electrode lesions and mPFC-LH cells and LH axon terminals
b. Representative images showing electrode lesions and mPFC-BLA cells and BLA axon terminals

c. Summary of mPFC optical fiber location (indicated with gray line), mPFC viral expression and LH CAV-Cre injection sites across mice for experiments shown below and in Fig 5. Distance to bregma is indicated under each brain slice. Top row shows LH and bottom row shows mPFC.
d. mPFC-LH photostimulation in ChR2 mice did not change latency to pick reward while performing reward task alone (n=10; paired t-test, p=0.42).
e. mPFC-LH photostimulation did not increase chow eating in the homecage (eYFP n=8, ChR2 n=7; 2-way RM ANOVA no significant effect of light, virus or interaction).
f. mPFC-LH photostimulation in ChR2 mice did not change time spent in social chamber in the 3-chamber social interaction assay (n=10; paired t-test, p=0.79).
g. mPFC-LH photostimulation did not change anxiety-like behavior in the open field (ChR2 n=8, eYFP n=8; 2-way repeated measures (RM) ANOVA no significant effect of light, virus or interaction).
h. mPFC-LH photostimulation did not evoke conditioned placed preference or aversion (ChR2 n=5, eYFP n=5; 2-way RM ANOVA no significant effect of light, virus or interaction).
i. Effort based T-maze allows mice to choose between a low reward low effort arm or a high reward high effort arm in which they must climb a wall to obtain the reward.
j. mPFC-LH photostimulation did not increase high effort choice in the effort T-maze (ChR2 n=8, eYFP n=9; 2-way RM ANOVA no significant effect of light, virus or interaction for both 14 and 7 cm walls).